JPP Journal of Pharmacy and Pharmacology

JPP 2008, 60: 1473–1479

Received March 27, 2008
Accepted June 30, 2008
DOI 10.1211/jpp.60.11.0008
ISSN 0022-3573

New coumarin-based anti-inflammatory drug: putative antagonist of the integrins $\alpha_L\beta_2$ and $\alpha_M\beta_2$

Claudio Bucolo, Adriana Maltese, Francesco Maugeri, Keith W. Ward, Monica Baiula, Antonino Spartà and Santi Spampinato

Abstract

This study was conducted to investigate putative antagonism of integrin receptors $\alpha_M\beta_2$ and $\alpha_L\beta_2$ by a novel coumarin derivative (BOL-303225-A), its efficacy in-vivo after retinal ischaemia–reperfusion injury, and its bioavailability in rat plasma. A cellular adhesion assay in Jurkat and U937 cells, and a flow cytometry assay with an antibody against the β_2 subunit were conducted. BOL-303225-A bioavailability in rat plasma and the retinal levels of myeloperoxidase (MPO) after ischaemia–reperfusion injury were evaluated after oral administration (10 mg kg^{-1}). In-vitro cell viability assays revealed no cytotoxicity for BOL-303225-A over a wide dose range, and IC50 values of 32.3 ± 1.5 μM and 84.95 ± 2.3 μM were found for Jurkat and U937 cells, respectively. The drug showed specific binding to the $\alpha_M\beta_2$ and $\alpha_L\beta_2$ integrin receptors expressed by U937 and Jurkat cells, respectively, producing a fluorescence shift towards lower values in a concentration-dependent manner. The pharmacokinetic profile of BOL-303225-A exhibited rapid absorption following oral administration in the rat. A significant reduction of retinal MPO levels was observed in drug-treated rats. This study demonstrated that BOL-303225-A acts as an antagonist of the integrin $\alpha_L\beta_2$ and $\alpha_M\beta_2$ receptors, suggesting that this drug could be used for ocular diseases such as diabetic retinopathy.

Introduction

Coumarins comprise a very large class of phenolic substances found in plants and the prototypical compound is coumarin itself, also known as 1,2-benzopyrone. The pharmacological promiscuity of interesting coumarins obtained from plants is well-depicted by the properties of scoparone (6,7-dimethoxycoumarin), which has been extensively investigated for its immunosuppressive, vascular relaxant and lipid-lowering activity (Huang et al 1993). Other coumarins such as osthole [7-methoxy-8(3-methylpent-2-enyl)coumarin], an active principle isolated from a Chinese plant, possess anti-inflammatory properties and inhibit platelet aggregation and thromboxane formation (Ko et al 1989). Diabetic retinopathy has an underlying inflammatory component, manifesting leukocyte recruitment and adhesion to the retinal vasculature and up-regulation of inflammatory genes. The retinal vasculature of diabetic humans contains increased numbers of leukocytes, a finding that coincides with the increased expression of intercellular adhesion molecule-1 (ICAM-1) in retinal vasculature (McLeod et al 1995). The phenomenon is also present in diabetic animal models and occurs whether the diabetes is spontaneous in nature or is induced (Schröder et al 1991; Miyamoto et al 1998, 1999). The increased density of leukocytes in the retinal vasculature begins as early as 1 week following the onset of experimental diabetes and results in injury to the endothelium, leading to a breakdown of the blood–retinal barrier (Joussen et al 2001, 2003). Blood–retinal barrier breakdown develops early in the course of diabetic retinopathy in humans and, as a long-term lesion, is the major pathology leading to macular oedema and the risk of subsequent visual loss. The leukocytes that adhere to the diabetic retinal vasculature use specific adhesion molecules such as the integrin ligand CD18, which forms the invariable portion of the heterodimers Mac-1 (CD11a/CD18) ($\alpha_M\beta_2$) and LFA-1 (CD11b/CD18) ($\alpha_L\beta_2$) (Barouch et al 2000). Leukocytes use CD18 to tether themselves to ICAM-1 on the surface of diabetic retinal vasculature. Previous work has established the role of CD18/ICAM-1 leukocyte adhesion in the pathogenesis of early diabetes-induced leukostasis and blood–retinal barrier breakdown (Joussen et al 2001).

Department of Experimental and Clinical Pharmacology, School of Medicine, University of Catania, Catania, Italy

Claudio Bucolo, Adriana Maltese, Francesco Maugeri

Global Preclinical Development, Bausch & Lomb, Rochester, NY, USA

Keith W. Ward

Department of Pharmacology, University of Bologna, Bologna, Italy

Monica Baiula, Antonino Spartà, Santi Spampinato

Correspondence: Claudio Bucolo, Department of Experimental and Clinical Pharmacology, School of Medicine, University of Catania, Viale A. Doria 6, 95125 Catania, Italy. E-mail: bucocla@unict.it

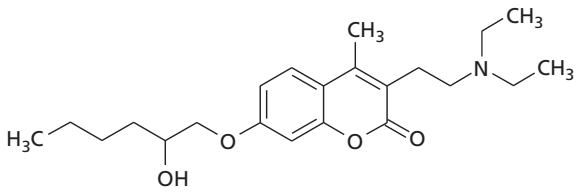

Figure 1 Two-dimensional chemical structure of BOL-303225-A.

In view of these mechanisms in the pathogenesis of diabetic retinopathy, a novel coumarin derivative, 3-(2-diethylamino-ethyl)-7-(2-hydroxy-hexyloxy)-4-methyl-chromen-2-one (BOL-303225-A; Figure 1), has been prepared to evaluate its pharmacological activity and specificity toward the integrin receptors $\alpha_M\beta_2$ and $\alpha_L\beta_2$. To date, no information concerning the putative antagonism effect against integrin receptors $\alpha_M\beta_2$ and $\alpha_L\beta_2$ is available for coumarin derivatives. Therefore, in this study we examined the ability of BOL-303225-A to compete with the binding of the integrin receptors $\alpha_L\beta_2$ and $\alpha_M\beta_2$, constitutively expressed by Jurkat E6.1 and U937 cells, respectively, to immobilized ligands such as ICAM-1 or fibronectin. Through adhesion assays we generated concentration–response curves to calculate the IC50 of this compound, while the specificity of action was evaluated by flow cytometry assays using anti-α_L, anti-α_M and anti-β_2 antibodies. In this study we also evaluated the pharmacokinetic profile of BOL-303225-A in rat plasma following oral administration of a single dose, to help place the pharmacological profile of the drug into a potentially therapeutic context. An in-vivo efficacy study was further conducted in rats to investigate the inhibitory effect of the drug on retinal leukocyte infiltration after ischaemia–reperfusion injury.

Materials and Methods

Chemicals and reagents

BOL-303225-A (HCl salt) was obtained from Bausch & Lomb (Rochester, New York, USA). The 96-well flat-bottom polystyrene non-treated plates were purchased from Costar (Sigma-Aldrich, Milan, Italy), recombinant human ICAM-1 was from R&D Systems (Minneapolis, MN, USA), Hank's balanced salt solution (HBSS), RPMI-1640 and bovine serum albumin (BSA) were from Cambrex Profarmaco (Milan, Italy), 5-chloromethylfluorescein diacetate was from Invitrogen (Carlsbad, CA, USA), Jurkat clone E6.1 cells and U937 cells were from the European Collection of Cell Cultures (ECACC Wiltshire, UK), fetal bovine serum (FBS) and phosphate-buffered saline (PBS) were from Biowhittaker (Milan, Italy), anti-CD49d antibody was from Calbiochem (Nottingham, UK), anti-CD18, anti-CD11a and anti-CD11b/CD18 were from Chemicon (Milan, Italy), and FITC-conjugated secondary antibody was from Molecular Probes, Invitrogen (Milan, Italy). Polyvinylpyrrolidone (PVP), acetonitrile, *n*-hexane, dichloromethane and triethylamine were purchased from Merck (Milan, Italy). Phorbol 12-myristate 13-acetate (PMA), fibronectin, Triton-X-100, 85% orthophosphoric acid, 37% w/w hydrochloric acid, sodium hydroxide, boric acid, sodium chloride, EDTA, Tris, glycine, phenylmethylsulfonyl fluoride, leupeptine and aprotinine were purchased from Sigma-Aldrich (Milan, Italy). All chemicals were of analytical or HPLC grade.

Animals

Male Sprague–Dawley rats (Morini, Reggio Emilia, Italy), 200–220 g, were used. The animals were housed in standard conditions, with a constant temperature (22 ± 1°C), relative humidity (30%) and under a constant light–dark cycle (lights on between 0800 and 2000 hours). Standard food and tap water were freely available. All experiments were carried out according to the Association for Research in Vision and Ophthalmology resolution on the use of animals in research and according to the Institutional Animal Care and Use Committee of the University of Catania.

Integrin $\alpha_L\beta_2$ and $\alpha_M\beta_2$ adhesion assay

Jurkat or U937 cells were used in this study. Jurkat cells are an immortalized line of T lymphocyte cells that constitutively express the integrin receptor $\alpha_L\beta_2$. U937 cells are human leukaemic monocyte lymphoma cells that constitutively express the integrin receptor $\alpha_M\beta_2$. Jurkat or U937 cells were grown in RPMI-1640 supplemented with 10% FBS. For Jurkat cells, FBS was heat-inactivated at 55°C for 30 min. At 48 h before the assay, 40 ng mL^{-1} PMA was added to the culture medium to stimulate integrin expression (Geiger et al 2000; Lishko et al 2004). The 96-well plates were coated with ICAM-1 (5 μg mL^{-1}) overnight at 4°C and the non-specific binding sites were blocked by incubation with HBSS/1% BSA (w/v) solution for 30 min at 37°C. A post-coating with 0.5% or 1% PVP for 1 h at 37°C was performed where indicated. The day of the assay, the cells were counted and stained with 12.5 μM 5-chloromethylfluorescein diacetate. After three rinses with HBSS/BSA solution, aliquots of 0.5×10^6 cells were divided in a number of tubes correspondent to the number of treatments until the cells in the control well were sufficiently removed. For inhibition experiments, cells were mixed with the drug and pre-incubated at 37°C for 30 min. The cell suspension was then transferred to the coated wells (100 μL in quadruplicate). After 30 min incubation, the non-specifically bound cells were washed away with HBSS/BSA. Finally, 50 μL of lysis buffer (0.5% Triton-X-100 in PBS) was added to the wells and incubated for 30 min at 4°C. Fluorescence was measured with a Victor^2 Wallac-1420 multilabel counter and the number of adherent cells was determined by interpolation with the standard curve. The efficacy of putative antagonist was determined by the decrement of adherent cells as compared with the control.

Cell viability assay

Cells were harvested and counted, then aliquoted in microtubes at a concentration of 0.5×10^6 cells. After centrifugation, the cells were resuspended in HBSS/BSA buffer containing different concentrations of the compound. After 60 min incubation, cell suspension and trypan blue solution were mixed together and counted using a

haemocytometer. The percentage of viable cells was calculated as follows:

% of living cells = (number of viable cells/total number of cells (dead and viable)) × 100

Flow cytometry assay

Fluorescence-activated cell sorting (FACS) analysis was performed to characterize the specificity of action of the drug on the integrin receptors. Cells were harvested, counted, and aliquoted at a concentration of 5×10^5 cells per tube. After one wash with HBSS/1% BSA, cells were incubated with a range of concentrations of the drug for 30 min at 37°C in a 5% CO_2 humidified atmosphere. Cells were then washed and incubated with 0.5 μg/sample of the primary antibody against $\alpha_L\beta_2$ and $\alpha_M\beta_2$ integrins for 30 min at 4°C. After two washings, the cells were incubated with the FITC-conjugated secondary antibody for 45 min at 4°C. Non-specific fluorescence was evaluated, analysing the binding of FITC-conjugated secondary antibody without adding primary antibody. Finally, the cells were washed and resuspended in HBSS/BSA buffer, ready to be analysed in an EPICS ELITE (Beckman Coulter, Inc., Rome, Italy) flow cytometer. For each sample, at least 10 000 events were collected. Many studies report that a reduction in cell size and buoyant density accompany apoptotic cell death: thus, apoptotic cells appear smaller and more dense than their normal counterparts. These changes are accurately detected by flow cytometry. The forward scatter, which indicates cell size, and the side scatter, which reveals the degree of granularity of the cell, were used to assess cell morphology (Darzynkiewicz et al 1994). The percentage of cells included within the gate area of control cells corresponds to viable cells and is reported.

In-vivo pharmacokinetic study

A total of 28 rats were randomly allocated into seven groups (four animals per group). BOL-303225-A (dissolved in saline at a concentration of 2.5 mg free base equivalent mL^{-1}), was orally administered by a gavage needle connected to a positive displacement pipettor directly into the stomach, in a volume depending on the rat bodyweight, to obtain a dose of 10 mg kg^{-1}. At 5 min before each blood collection, each animal was deeply anesthetized with 0.1 mL of Zoletil-100 (50 mg mL^{-1} of Tiletamine·HCl and 50 mg mL^{-1} of Zolazepam·HCl) injected intraperitoneally. Then, at 15, 30, 60, 90, 120, 180 and 240 min after the administration of the drug, a cardiac puncture with a 23-G needle was performed and a maximum volume of blood was withdrawn to exsanguinate the animal. Blood samples were collected into heparinized tubes. Plasma samples were obtained from blood samples by centrifugation at 3000 *g* for 5 min and stored at –20°C until the HPLC analysis for a period not longer than 2 weeks. Concentrations of BOL-303225-A in the above plasma samples were analysed by HPLC according to the method previously described by Maltese et al (2007).

Retinal ischaemia–reperfusion injury

A total of 18 rats were randomly divided into three groups (six animals per group): ischaemic rats BOL-303225-A treated, ischaemic rats saline treated, and non-ischaemic rats as control. BOL-303225-A (10 mg kg^{-1}) or saline was orally administered, as described above, immediately before and 2 h after the retinal ischaemia induction. The rats were anaesthetized with 0.1 mL of Zoletil-100 injected intraperitoneally. To induce retinal ischaemia, the anterior chamber of the right eye was cannulated with a 25-gauge infusion needle connected by silastic tubing to a saline reservoir. The intraocular pressure of the cannulated eye was raised to 110 mmHg for 45 min by elevating the saline reservoir. Then the cannula was removed, and reperfusion of the retina vessels was confirmed by ophthalmoscopy. At 24 h after reperfusion the animals were killed by CO_2 inhalation and the right eyeball of each animal was enucleated. To evaluate the infiltration of leukocytes in retina and vitreous, an MPO enzyme-linked immunosorbent assay kit (HBT, Uden, The Netherlands) was used. Immediately after killing, the retina and vitreous were collected as a whole from enucleated eyes, accurately weighed, and sonicated in 2 mL of lysis buffer (200 mM NaCl, 5 mM EDTA, 10 mM Tris, 10% glycine, 1 mM PMSF, 1 μg mL^{-1} leupeptine and 28 μg mL^{-1} aprotinine; pH 7.4). The homogenate was centrifuged twice (1500 *g* at 4°C for 15 min) to avoid contamination of cell debris and the supernatants were stored at –80°C until analyses. Homogenate samples were treated following the assay procedure described in the kit and a microplate reader (model DV 990 B/V6: GDV, Rome, Italy) set at 450 nm was used for the analysis.

Statistical analysis

Statistical analyses were performed using GraphPad Prism version 4.0 for Windows (GraphPad, San Diego, CA, USA). For MPO analysis, a one-way analysis of variance followed by a Newman–Keuls post-hoc test was performed ($P < 0.05$ was considered statistically significant). Pharmacokinetic parameters were calculated using WinNonlin version 5.0.1 software (Pharsight Corporation, Mountain View, CA, USA). The area under the curve (AUC) and the area under the first moment curve (AUMC) for plasma BOL-303225-A concentrations versus time, from 0 to 240 min and from 0 extrapolated to infinity, were calculated using the trapezoidal rule. The maximal plasma concentration (C_{max}) and the time to reach C_{max} (T_{max}) were determined directly from the plasma concentration–time curve. The mean residence time was calculated by dividing the AUMC by AUC. The first-order rate constant associated with the terminal (log-linear) elimination phase (λ_Z) of the plasma concentration–time curve was calculated from the linear portion of the concentration versus time profile. All data are presented as mean ± s.d.

Results

In-vitro study

A trypan blue cell viability assay was performed to evaluate if the active concentrations of BOL-303225-A were toxic for the cells. The cell viability assay demonstrated that the active drug concentration range (from 0.001 to 1 mM) was not toxic

for Jurkat and U937 cells (data not shown). These results were confirmed by cell morphology assessed by flow cytometry analysis as previously described (Vizler et al 2002; Hopkinson et al 2007). Figure 2 shows flow cytometry performed on U937 cells gated on the basis of their forward and side light scatter. Similar results were obtained for Jurkat cells (data not shown). BOL-303225-A only at the highest concentration tested (1.25 mM) showed a modification in cell morphology (Figure 2); this concentration is well above those required for efficacy.

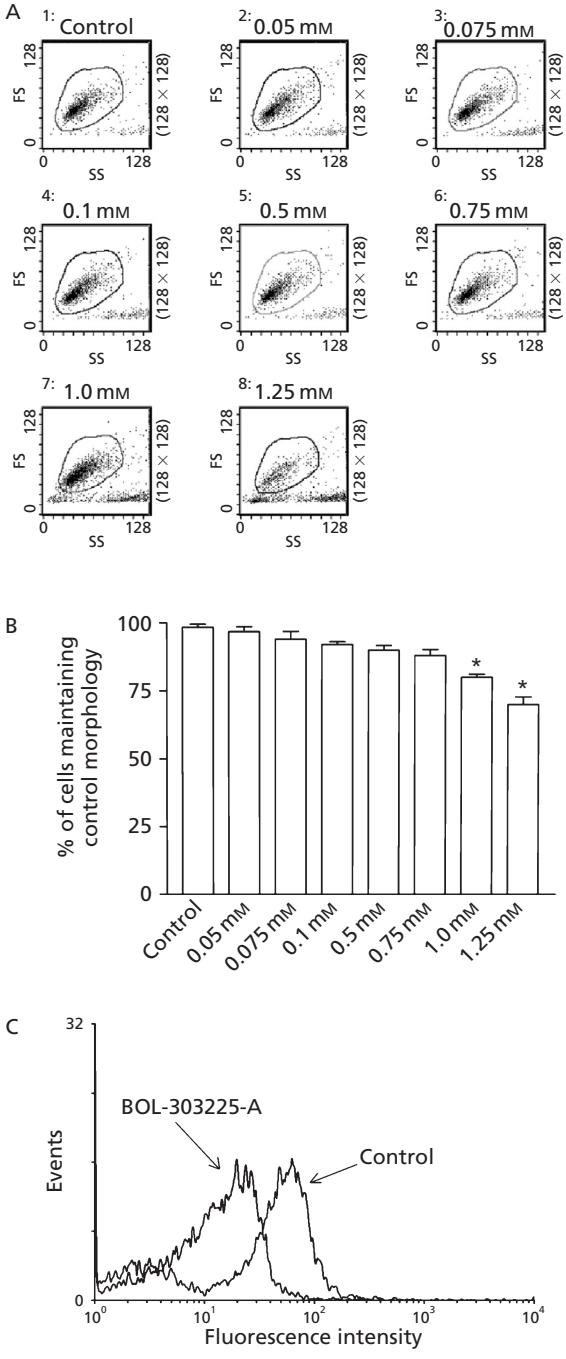

Figure 2 Flow cytometry assay of U937 cells exposed to increasing concentrations of BOL-303225-A (A). The percentage of cells maintaining control morphology and corresponding to viable cells is indicated within each frame. Mean values ± s.e.m. of % cells maintaining control morphology are reported. *$P < 0.01$, significantly different compared with control (Newman-Keuls test after analysis of variance), n = 3 (B). Shift of fluorescence to lower values (C) induced by BOL-303225-A (0.1 mM) compared with control U937 cells.

Jurkat cells expressing the integrin $\alpha_L\beta_2$ underwent adhesion assays on 96-well plates coated with ICAM-1. A saturation curve with different concentrations of the ligand was performed (data not shown), and a concentration of 5 μg mL^{-1} was chosen. Jurkat cells were assayed with a range of concentrations of the putative integrin antagonist BOL-303225-A. An IC50 value of 32.3 ± 1.5 μM (n = 3) was calculated for BOL-303225-A (Figure 3). Similarly, we performed the adhesion assay on U937 cells expressing the integrin $\alpha_M\beta_2$ (Figure 3). ICAM-1 is considered a selective ligand for this receptor, but, because of its very low surface expression in the wild-type strain and the limited genic induction and avidity augmentation induced by PMA (Lishko et al 2001; Hamada & Utiyama 2005), we preferred to coat the plates with fibronectin, followed by a post-coating with 1% PVP (w/v) in water. The cells adhered readily to fibronectin (10 μg mL^{-1}) in a seeding concentration fashion, whereas their behaviour toward ICAM-1 at a coating concentration as high as 5 μg mL^{-1} was not distinguishable from the background (data not shown).

The $\alpha_M\beta_2$ integrin is a promiscuous receptor that is able to bind to fibronectin as reported by Lishko et al (2003), and it is unlikely, in our case, that it is the only intervening receptor in U937 adhesion to the coated well. Therefore, it is not surprising that we calculated higher values of IC50 than in the Jurkat cell experiment (84.95 ± 2.3 μM), probably due to the cooperation of a wider typology of integrin receptors. However, BOL-303225-A was able to prevent cell adhesion in a concentration-dependent manner, demonstrating good potency. In a similar fashion, previous adhesion studies carried out in our laboratory with cloricromene, a well-known coumarin derivative, showed that the IC50 was 515 ± 23 μM and 1232 ± 59 μM with Jurkat cells and U937 cells, respectively (unpublished data).

To demonstrate the specificity of the action of the new coumarin derivative drug on the integrin receptors, we

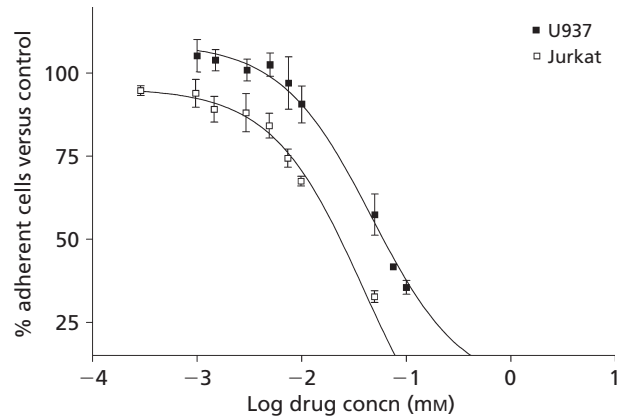

Figure 3 Comparison of the effect of BOL-303225-A on U937 adhesion on fibronectin (■) and on Jurkat adhesion on ICAM-1 (□).

performed a displacement flow cytometry assay with the antibody against the β_2 subunit. BOL-303225-A showed specific binding to the $\alpha_M\beta_2$ integrin receptor expressed by U937 cells (Figure 2), as well as to the $\alpha_L\beta_2$ integrin receptor expressed by Jurkat cells (data not shown), producing a fluorescence shift towards lower values in a concentration-dependent manner. When the cells were treated with BOL-303225-A and exposed to the antibody, the fluorescence intensity decreased due to the drug binding to the integrin receptor blocking the FITC-conjugated antibody binding.

In-vivo study

The plasma concentration–time profile of BOL-303225-A after oral administration (10 mg kg^{-1}) to healthy rats is illustrated in Figure 4, and the calculated pharmacokinetic parameters are shown in Table 1. BOL-303225-A exhibited rapid absorption following oral administration in the rat, with maximal concentrations achieved at the first sampling point. Plasma sampling through 4 h post-dose captured the majority of the concentration–time profile, with only 16% of the AUC extrapolated from the last sampling time to infinity. Based on these data, BOL-303225-A appears to demonstrate a half-life of approximately 1.8 h following oral administration in the rat.

Figure 5 indicates the levels of MPO in the vitreoretinal complex. A significant reduction of vitreoretinal MPO levels was observed in the BOL-303225-A treated rats compared with the saline treated group.

Discussion

A pharmacological profile of a new coumarin derivative, BOL-303225-A, was assessed in the current study. We found that this drug reduced retinal leukostasis acting as an antagonist of $\alpha_L\beta_2$ and $\alpha_M\beta_2$ integrins. BOL-303225-A is a synthetic coumarin derivative with a chemical structure similar to cloricromene, one of the most well-studied coumarin-based anti-inflammatory drugs (Cuzzocrea 2000; Bucolo 2003), but with greater potency and less toxicity (unpublished data). A combination of antithrombotic/vasorelaxant properties has been demonstrated for cloricromene (Squadrito et al 1991). Cloricromene has been extensively evaluated in several in-vitro and in-vivo studies, suggesting that it may act through tumour necrosis factor α (TNF-α) inhibition. Hence, it has been recently demonstrated that cloricromene inhibits lipopolysaccharide (LPS)-induced TNF-α transcription and nuclear factor-κB (NF-κB) activation in rat alveolar macrophages (Corsini et al 2001). Further, Ianaro et al (2004) showed that cloricromene protects rats from LPS by blocking LPS-induced NF-κB activation, leading to inhibition of nitric oxide and TNF-α overproduction. More recently, we demonstrated (Bucolo et al

Table 1 Pharmacokinetic parameters of BOL-303225-A obtained by non-compartmental analysis

Pharmacokinetic parameters	
C_{max} (μg mL^{-1})	1.04 ± 0.55
T_{max} (min)	15.00
AUC_{0-240} (min μg mL^{-1})	38.04
$AUC_{0-\infty}$ (min μg mL^{-1})	43.95
$AUMC_{0-\infty}$ (min^2 μg mL^{-1})	4630.07
$MRT_{0-\infty}$ (min)	105.34
λ_Z (min^{-1})	0.0063
t½ (min)	109.72
Vd/F (mL kg^{-1})	36352.74
CL_t/F (mg min^{-1} kg^{-1})	229.66

C_{max}, maximal observed drug concentration; T_{max}, time at which C_{max} is observed; AUC, area under the plasma drug concentration–time curve; AUMC, total area under the first moment–time curve; MRT, mean residence time; λ_Z, exponential coefficient; t½, half-life; Vd/F, apparent volume of distribution; CL_t/F, apparent total clearance, where F represents oral bioavailability.

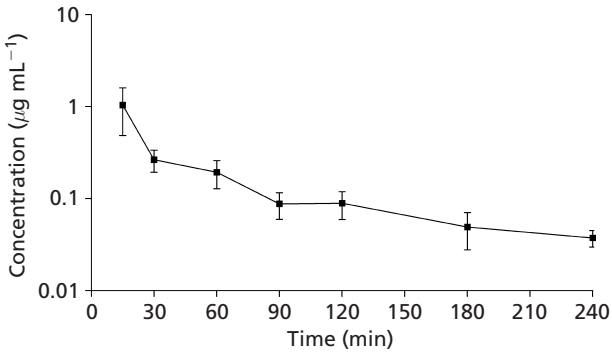

Figure 4 Plasma concentration–time profile of BOL-303225-A after oral administration (10 mg kg^{-1}) to healthy rats. Values represent the concentration of the drug as free base and are expressed as mean ± s.d., n = 4.

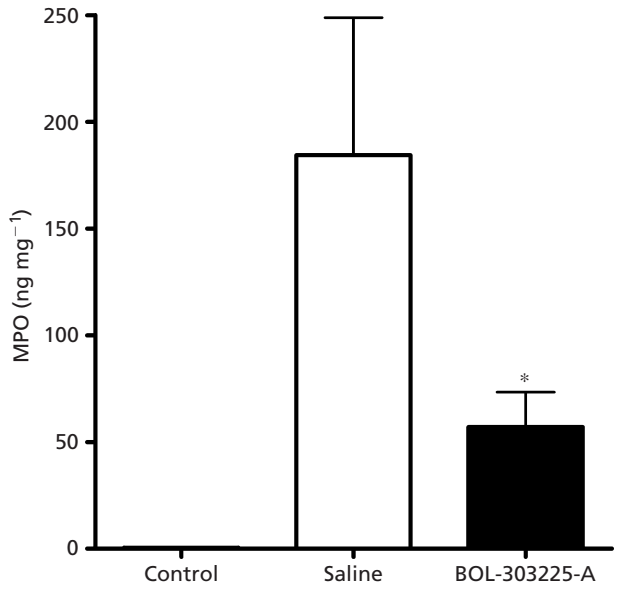

Figure 5 Myeloperoxidase (MPO) levels in rat vitroretinal complex 24 h after ischaemia induction. Values are expressed as mean ± s.d., n = 6. Control: normal eye, no ischemia. *$P < 0.01$, significantly different compared with saline.

2003) that cloricromene attenuates the uveitis induced by endotoxin in the rat, reducing the inflammatory process and inhibiting, among others, the P-selectin and the ICAM-1. It is evident that coumarins possess a variety of pharmacological and biochemical properties, some of which may be of potential pharmaceutical interest for the treatment of ocular diseases.

Diabetic retinopathy, among other ocular diseases, remains a leading cause of vision loss and blindness. Much of the retinal damage that characterizes the diabetic retinopathy results from vascular leakage and ischaemia. These features are associated with retinal leukocyte stasis that is correlated with the increased expression of adhesion molecules and integrins. The $\alpha_L\beta_2$ and $\alpha_M\beta_2$ integrins play an important role in the pathogenesis of diabetic retinopathy, therefore pharmacological antagonism of $\alpha_L\beta_2$ and $\alpha_M\beta_2$ is an attractive approach for the treatment of this disease. In this study, we showed, for the first time, that the synthetic coumarin derivative BOL-303225-A acts as putative antagonist of the integrin $\alpha_L\beta_2$ and $\alpha_M\beta_2$ receptors, and it is able to significantly decrease the polymorphonuclear leukocyte levels in the retinal tissue. Similarly, U937 cells have been our viable model for the $\alpha_M\beta_2$ integrin receptor adhesion studies. Since in this cell line the binding to ICAM-1 was not enhanced by phorbol ester stimulation, we deemed fibronectin a suitable immobilized ligand for our purposes. Fibronectin is less selective for the $\alpha_M\beta_2$ receptor than ICAM-1, therefore, supported by the data acquired, we expected a reduced potency of the drugs in their ability to decrease cell adhesion to the coated plates. FACS investigations with anti-α_M and anti-β_2 antibodies supported the binding specificity of the drugs to this integrin. The binding specificity evaluated by flow cytometry assay showed that BOL-303225-A binds to $\alpha_L\beta_2$ and $\alpha_M\beta_2$ integrin receptors. However, we cannot rule out the possibility that the compound binds to other integrin recognition sites, a point that will be further investigated in future studies.

In the rat pharmacokinetic study with BOL-303225-A, a C_{max} of approximately 2.5 μM was achieved following a 10-mg kg^{-1} oral dose. BOL-303225-A demonstrated a very high apparent volume of distribution, Vd/F (36 L kg^{-1}), and although absolute F is not known, it is possible that this Vd would be consistent with good tissue distribution of the compound, such that tissue concentrations may be greater than the plasma levels reflected in this experiment. Rats are often a reasonable model for human pharmacokinetics (Ward et al 2005), although the ability to extrapolate rat pharmacokinetics to the human situation is dependent on the physicochemical features of the compound of interest (Jolivette & Ward 2005). For BOL-303225-A, which has an estimated cLogP of approximately 4.7, it is possible that high clearance in the rat would not be predictive of high clearance in humans; further pharmacokinetic studies in other species would be useful in estimating the likely human exposure to this drug.

In conclusion, the results suggest that BOL-303225-A is a putative antagonist of the integrin $\alpha_L\beta_2$ and $\alpha_M\beta_2$ receptors. In addition, it is noteworthy that this new chemical entity reaches the IC50 at concentrations that do not show cytotoxicity. Along with the preliminary pharmacokinetic data from this study, these observations suggest that the utility of BOL-303225-A as a potential treatment for diseases such as diabetic retinopathy should be further investigated.

References

Barouch, F. C., Miyamoto, K., Allport, J. R., Fujita, K., Bursell, S. E., Aiello, L. P., Luscinskas, F. W., Adamis, A. P. (2000) Integrin-neutrophil adhesion and retinal leukostasis in diabetes. *Invest. Ophthalmol. Vis. Sci.* **41**: 1153–1158

Bucolo, C., Cuzzocrea, S., Mazzon, E., Caputi, A. P. (2003) Effects of cloricromene, a coumarin derivative, on endotoxin-induced uveitis in Lewis rats. *Invest. Ophthalmol. Vis. Sci.* **44**: 1178–1184

Corsini, E., Lucchi, L., Binaglia, M., Viviani, B., Bevilaqua, C., Monastra, G., Marinovich, M., Galli, C. L. (2001) Cloricromene, a semi-synthetic coumarin derivative, inhibits tumor necrosis factor-alpha production at a pre-transcriptional level. *Eur. J. Pharmacol.* **418**: 231–237

Cuzzocrea, S., Mazzon, E., Bevilaqua, C., Costantino, G., Britti, D., Mazzullo, G., De Sarro, A., Caputi, A. P. (2000) Cloricromene, a coumarin derivative, protects against collagen-induced arthritis in Lewis rats. *Br. J. Pharmacol.* **131**: 1399–1407

Darzynkiewicz, Z., Li, X., Gong, J. (1994) Assays of cell viability: discrimination of cells dying by apoptosis. *Methods Cell Biol.* **41**: 15–38

Geiger, C., Nagel, W., Boehm, T., van Kooyk, Y., Figdor, C. G., Kremmer, E., Hogg, N., Zeitlmann, L., Dierks, H., Weber, K. S., Kolanus, W. (2000) Cytohesin-1 regulates beta-2 integrin-mediated adhesion through both ARF-GEF function and interaction with LFA-1. *EMBO J.* **19**: 2525–2536

Hamada, K., Utiyama, H. (2005) Functional cytoplasmatic domains of the Mac-1 integrin receptor in phorbol ester-treated U937 cells. *Biochem. Biophys. Res. Commun*. **335**: 858–864

Hopkinson, K., Williams, E. A., Fairburn, B., Forster, S., Flower, D. J., Saxton, J. M., Pockley, A. G. (2007) A MitoTracker Green-based flow cytometric assay for natural killer cell activity: variability, the influence of platelets and a comparison of analytical approaches. *Exp. Hematol.* **35**: 350–357

Huang, H. C., Weng, Y. I., Lee, C. R., Jan, T. R., Chen, Y. L., Lee, Y. T. (1993) Protection by scoparone against the alterations of plasma lipoproteins, vascular morphology and vascular reactivity in hyperlipidaemic diabetic rabbit. *Br. J. Pharmacol*. **110**: 1508–1514

Ianaro, A., Maffia, P., Grassia, G., Di Meglio, P., Sorrentino, R., di Villa Bianca, R., Di Rosa, M., Ialenti, A. (2004) Cloricromene in endotoxemia: role of NF-κB. *Naunyn Schmiedebergs Arch. Pharmacol*. **370**: 140–145

Jolivette, L. J., Ward, K. W. (2005) Extrapolation of human pharmacokinetic parameters from rat, dog, and monkey data: molecular properties associated with extrapolative success or failure. *J. Pharm. Sci.* **94**: 1467–1483

Joussen, A. M., Murata, T., Tsujikawa, A., Kirchhof, B., Bursell, S. E., Adamis, A. P. (2001) Leukocyte-mediated endothelial cell injury and death in the diabetic retina. *Am. J. Pathol.* **158**: 147–152

Joussen, A. M., Poulaki, V., Mitsiades, N., Cai, W. Y., Suzuma, I., Pak, J., Ju, S. T., Rook, S. L., Esser, P., Mitsiades, C. S., Kirchhof, B., Adamis, A. P., Aiello, L. P. (2003) Suppression of Fas-FasL-induced endothelial cell apoptosis prevents diabetic blood-retinal barrier breakdown in a model of streptozotocin-induced diabetes. *FASEB J.* **17**: 76–78

Ko, F. N., Wu, T. S., Liou, M. J., Huang, T. F., Teng, C. M. (1989) Inhibition of platelet thromboxane formation and phosphoinositides breakdown by osthole from *Angelica pubescen*. *Thromb. Haemost.* **62**: 996–999

Lishko, V. K., Yakubenko, V. P., Hertzberg, K. M., Grieninger, G., Ugarova, T. P. (2001) The alternatively spliced alpha(E)C domain of human fibrinogen-420 is a novel ligand for leukocyte integrins alpha(M)beta(2) and alpha(X)beta(2). *Blood* **98**: 2448–2455

Lishko, V. K., Yakubenko, V. P., Ugarova, T. P. (2003) The interplay between integrins alphaMbeta2 and alpha5beta1 during cell migration to fibronectin. *Exp. Cell. Res*. **283**: 116–126

Lishko, V. K., Novokhatny, V. V., Yakubenko, V. P., Skomorovska-Prokvolit, H. V., Ugarova, T. P. (2004) Characterization of plasminogen as an adhesive ligand for integrins alphaMbeta2 (Mac-1) and alpha5beta1 (VLA-5). *Blood* **104**: 719–726

Maltese, A., Maugeri, F., Ward, K. W., Bucolo, C. (2007) Development and validation of an RP-HPLC-UV method for the determination of BOL-303225-A, a new coumarin-based anti-inflammatory drug, in rat plasma. *Biomed. Chromatogr.* **21**: 351–355

McLeod, D. S., Lefer, D. J., Merges, C., Lutty, G. A. (1995) Enhanced expression of intracellular adhesion molecule-1 and P-selectin in the diabetic human retina and choroid. *Am. J. Pathol.* **147**: 642–653

Miyamoto, K., Hiroshiba, N., Tsujikawa, A., Ogura, Y. (1998) In vivo demonstration of increased leukocyte entrapment in retinal microcirculation of diabetic rats. *Invest. Ophthalmol. Vis. Sci.* **39**: 2190–2194

Miyamoto, K., Khosrof, S., Bursell, S. E., Rohan, R., Murata, T., Clermont, A. C., Aiello, L. P., Ogura, Y., Adamis, A. P. (1999) Prevention of leukostasis and vascular leakage in streptozotocin induced diabetic retinopathy via intercellular adhesion molecule-1 inhibition. *Proc. Natl Acad. Sci. USA* **96**: 10 836–10 841

Schröder, S., Palinski, W., Schmid-Schönbein, G. W. (1991) Activated monocytes and granulocytes, capillary nonperfusion, and neovascularization in diabetic retinopathy. *Am. J. Pathol*. **139**: 81–100

Squadrito, F., Prosdocimi, M., Altavilla, D., Zingarelli, B., Caputi, A. P. (1991) Cloricromene. *Cardiovasc. Drug Rev*. **9**: 357–371

Vizler, C., Nagy, T., Kusz, E., Glavinas, H., Duda, E. (2002) Flow cytometric cytotoxicity assay for measuring mammalian and avian NK cell activity. *Cytometry* **47**: 158–162

Ward, K. W., Erhardt, P., Bachmann, K. (2005) Application of simple mathematical expressions to relate the half-lives of xenobiotics in rats to values in humans. *J. Pharmacol. Toxicol. Methods* **51**: 57–64